Effects of pyrolysis and incineration on the phosphorus fertiliser potential of bio-waste- and plant-based materials

Waste Management 172 (2023) 358–367

Contents lists available at ScienceDirect

Waste Management

journal homepage: www.elsevier.com/locate/wasman

Research Paper

Effects of pyrolysis and incineration on the phosphorus fertiliser potential of bio-waste- and plant-based materials

James Stephen Robinson [a,*], Peter Leinweber [b]

[a] Department of Geography and Environmental Science, University of Reading, Reading RG6 6AB, UK
[b] Soil Science, Faculty for Agricultural and Environmental Sciences, University of Rostock, Justus-von-Liebig Weg 6, 18059 Rostock, Germany

ARTICLE INFO

Keywords:
Biomass feedstocks
Thermal treatment
Biochar
Ash
Phosphorus fertiliser potential

ABSTRACT

Land application of biomass materials and their products of thermal treatment (biochars and ashes) can offset the unsustainable use of soluble P fertilisers. However, few evaluations of P fertiliser potential have systematically addressed diverse biomass types with contrasting P contents.

This paper evaluates the relative P fertiliser potential of four P-rich biowastes (animal bone, poultry manure, pig slurry, and a municipal sewage sludge) and three low-P, plant-based materials (reeds [Phragmites australis L.], rice husks [Oryza sativa L.] and cocoa prunings [Theobroma cacao L.]) and their biochars and ashes. We utilised three complementary approaches: P extractability in single solvents (2% formic and citric acids, and 1 M neutral ammonium citrate); sequential chemical P fractionation, and P dissolution/desorption kinetics.

In most cases, pyrolysis and incineration of the P-rich biowastes increased P extractability (% TP) in the single solvents, whilst decreasing water-soluble P. For example, pyrolysis reduced water-soluble P 20-fold, with corresponding increases observed not only in the solvent-extractable P but also in the pool of potentially plant available, $NaHCO_3$-Pi fraction (e.g., 17 to 35% TP). These complementary datasets were also evident for the low-P feedstocks and thermal products; e.g., pyrolysis increased the $NaHCO_3$-Pi fraction in reed feedstock from 6 to 15% TP. For all biomass feedstocks, biochars and ashes, pseudo-second order P-release kinetics provided the best fit with the experimental data.

The data demonstrate scope for using pyrolysis to upgrade the P fertiliser value of a wide range of biomass materials whilst reducing their environmental impact.

1. Introduction

Increasing demands for food and bioenergy continue to exploit global reserves of economically extractable rock phosphate for the manufacture of conventional, refined phosphorus (P) fertilisers (Cordell and White, 2011; Ulrich and Frossard, 2014). Rising concerns about the depletion of these non-renewable P reserves demand strategies for more efficient use of secondary P resources as alternative fertilisers (Withers et al., 2015; Römer and Steingrobe, 2018).

Biomass materials have long been used as alternative, or organic, fertilisers. With regards to the potential for direct application to land of these materials, they generally fall into one of two categories: relatively P-rich bio-waste (e.g. livestock manures, municipal biosolids and bone meal) or high C-containing, plant-based, ligno-cellulosic materials (e.g. wood, grain husks, nut shells) (Robinson et al., 2018). Naturally, of the two categories, P-rich materials (≥0.5% P w/w) have received by far the most attention as effective sources of fertiliser P (e.g., Schroder, 2005). However, their rates and amounts of P release may exceed crop P needs. These localised imbalances between P supply and demand are usually attributed to highly soluble forms of P in certain manures, as well as application practices designed to meet the N rather than P demand of the crops; both scenarios can lead to the release and transport of excess P to surface water bodies, where it can contribute to eutrophication (Sharpley et al., 2001; Li et al., 2018). Therefore, in order to reduce the eutrophication risk from land-applied biowastes, it appears necessary to decrease the portion of water-soluble P.

Unlike biowastes, ligno-cellulosic materials have a characteristically low P content (≤0.5% P w/w), stable C-containing organic compounds and high C:P ratio. Fundamentally, these properties render most plant-based materials unsuitable for fertiliser use. Nonetheless, plant residues are widespread and generally accessible globally; for example, high yielding and harvestable perennial vegetation, and agricultural by-

* Corresponding author.
E-mail addresses: j.s.robinson@reading.ac.uk (J.S. Robinson), peter.leinweber@uni-rostock.de (P. Leinweber).

https://doi.org/10.1016/j.wasman.2023.10.012
Received 18 March 2023; Received in revised form 1 October 2023; Accepted 12 October 2023
Available online 10 November 2023

products that require sustainable means of disposal. If recycled for use as fertilisers, these wastes pose less of a threat to water quality. Moreover, the combination of P-recycling with longer-term C-storage in soil is known to contribute not only to climate change mitigation but also to general enhancement of soil fertility and health for crop production (e.g., Negassa et al., 2012). Essentially, some of these plant residues (e.g. reeds, grains, shells and husks) have relatively high-mineral contents, and earlier research indicates that they could provide suitable feedstocks for P supply in low-input agricultural systems with P-deficient soils (Zheng et al., 2013; Robinson et al., 2018). Nonetheless, central to enhancing the P recycling potential of these low-P materials would be an increase in their portion of plant-available P.

Thermal processes, such as incineration, pyrolysis and gasification, were developed primarily as technologies to produce renewable energy from biomass materials (McKendry, 2002; Cantrell et al. 2008). Typically, incineration and gasification occur in the presence of excess oxygen above 800 °C, while pyrolysis operates under a limited supply of oxygen and at relatively low temperatures (<700 °C). Additional benefits of thermal processing include the removal of organic pollutants and pathogens from the biomass, whilst retaining and concentrating the mineral P content of the solid by-product; essentially, these transformations increase the product's P recycling options (Chan and Xu, 2009; Christel et al. 2014). However, whilst producing a more stable and storable fertiliser product that might promise a more precise application rate in the field, thermal processing also exerts a marked and varied influence on the forms and solubility of the P by modifying the biomass feedstock's physical and chemical structures. These modifications may result in highly variable P fertiliser efficiency among processed materials, potentially offsetting their economic and environmental advantages. For example, incineration of bone meal and sewage sludge produces high yields of calcium phosphate-rich ash, but typically converts the P compounds to more crystalline and less water-soluble forms, which reduces the value of the ashes as P fertiliser in comparison to the original feedstock (Thygesen et al., 2011; Komiyama et al., 2013). Conversely, reports suggest that pyrolysis treatments at low-to-moderate temperatures (400–500 °C) may favour the net accumulation of potentially useful proportions of plant available P; these changes have been observed during pyrolysis both of P-rich manures and relatively low-P, ligno-cellulosic plant residues (Christel et al., 2014; Uchimiya and Hiradate, 2014; Xu et al., 2016; Li et al., 2018). Indeed, some workers have shown that P in manure biochar can contribute more plant-available P than inorganic P fertilizers (Gunes et al. 2014).

There have been relatively few evaluations of secondary resource P fertilisers that address the full diversity of potentially accessible feedstocks and the products of their thermal treatment. Although plant bioassays can provide directly relevant data on the P fertiliser equivalence of these materials, the methods are time consuming and expensive. As an alternative, the solubility of P, obtained using chemical and / or aqueous extraction procedures, can provide a simple and indirect approach to predict P availability. The solubility of P in solvents such as 2% formic acid, 2% citric acid, and 1 M neutral ammonium citrate is traditionally used in the fertiliser industry to predict the P availability of phosphate rock (Rajan et al. 1992) and, more recently, biochar and ash derived from mineral-rich feedstocks; e.g. biosolids, manure and bone (Wang et al. 2012; Christel et al., 2014; Zwetsloot et al., 2014; Kratz et al., 2019). The theoretical justification for using these solvents rests on the influence of soil pH and organic ligands on dissolution, desorption and complexation reactions that can release *ortho*-P to the soil solution. As an alternative to single solvents, a sequence of strong alkali and acid solutions can be used for the indirect evaluation of P fertiliser potential. For example, Leinweber et al. (1997), Qian and Jiang (2014) and Kahiluoto et al. (2015) adopted the soil P fractionation scheme of Hedley et al. (1982) to characterise P in a range of animal manures and sewage sludge. More recently, similar schemes have been applied to the biochars and ashes of a variety of biowaste and plant-based materials (Qian and Jiang, 2014; Xu et al., 2016; Li et al., 2018). Whilst valuable as routine or preliminary indicators of secondary resource P fertiliser potential, a common criticism of standard chemical extraction and fractionation procedures is their static, or non-equilibrium, mode of operation. A further approach to assessing potential P fertiliser is through an evaluation of the kinetics of the materials' P solubility. Some workers have adopted this approach to the investigation of biochars of low-P biomass, e.g. rice husks and giant reeds (Qian et al., 2013; Zheng et al., 2013); whilst others have focused on manures (Liang et al., 2017; Tran et al., 2017).

To the best of our knowledge, the P fertiliser potential of biomass materials with contrasting P contents have not yet been systematically evaluated in a single study. The current paper addresses this research gap by investigating the relative P solubility characteristics of a diverse range of biowaste- and plant-based feedstocks, as well as their biochars and ashes derived from pyrolysis and incineration, respectively.

2. Material and methods

2.1. Feedstocks

Seven biomass feedstocks were selected for this study. Four of the feedstocks were bio-wastes: animal bone [BONE]; poultry manure [POUL]; pig slurry [PIG], and an anaerobically digested, municipal sewage sludges [BIOS]. The other three feedstocks were plant-based materials: wetland reed (Phragmites australis L.) [REED]; rice husks (Oryza sativa L.) [RICE] and cocoa prunings (Theobroma cacao L.) [COCA].

Defatted animal bone chips (C-quality, 2 to 5 mm size) were purchased from Sonac Ltd. Vuren, Netherlands. The poultry manure was obtained from a broiler chicken farm in Vilnius, Lithuania. The pig slurry, obtained from a swine unit in the Netherlands, was membrane-filtered to a dry matter content of 98 % (w/w). Samples of anaerobically digested, dewatered and conditioned sewage sludge were collected from a municipal wastewater treatment centre in the UK (Reading) (BIOS). The reed samples originate from newly established paludiculture in the Mecklenburg-Western Pommerania lake distric (Lakes Malchin and Kummerow) and were delivered by a local company in Mecklenburg-Western Pomerania (Biotherm Hagenow GmbH). To facilitate handling, the long fibres were shredded and pelletized. The rice husks were collected from Indonesia, and the cocoa prunings (young shoot cuttings) from a small-holder, agro-forestry operation in Ecuador.

2.2. Biochar and ash preparation

Biochars were produced by pyrolysis of the feedstocks in industry-scale installations under N_2 flow, between 480 and 500 °C, with solid residence times of between 10 and 20 min (M.E.E. EREKA and EPI Bioreactors, Germany and UK). Ash was produced by incineration in a muffle furnace at 850 °C for 5 h. A portion of each feedstock, biochar and ash sample was dried at 60 °C overnight and ground to pass a 125-μm sieve (120-mesh) in preparation for the subsequent elemental analysis and experiments.

2.3. Elemental analysis and pH determination

All solid material total C and N were determined by a CN analyser (Vario EL III; Elementar Analysensysteme, Hanau, Germany), and total P, K, Ca, Mg, Fe and Al by inductively coupled plasma optical emission spectroscopy (ICP OES) (JY 238 UL Trace, France) after microwave-assisted digestion in concentrated nitric acid and 30% hydrogen peroxide (USEPA, 1996). The pH of all materials was measured in a 10% (w/v) suspension in deionised water prepared by shaking at 100 rpm for 1 h at 25 °C.

Table 1
Elemental composition (g kg^{-1}) and pH of the biomass feedstocks and their derived biochars and ashes.

Sample	C	N	P	K	Ca	Mg	Fe	Al	pH
Bio-waste									
BONE	178	50.5	104	1.3	195	4.1	0.1	0.0	7.2
BONE-B*	104	18.6	129	1.9	238	5.5	0.1	0.1	8.7
BONE-A*	69.2	16.4	203	2.9	397	7.8	0.2	0.1	9.4
POUL	347	44.6	12.6	17.9	60.1	6.4	1.0	0.1	7.5
POUL-B	311	28.1	35.1	49.1	132	17.5	2.2	0.4	9.2
POUL-A	57.4	1.8	45.2	46.0	191	22.4	2.9	0.2	11.8
PIG	378	26.9	20.4	13.7	25.1	13.1	5.6	0.9	8.0
PIG-B	381	22.8	50.9	30.3	56.7	33.0	15.9	2.5	8.8
PIG-A	17.4	0.2	92.5	54.6	103	53.2	21.8	3.3	10.7
BIOS	399	34.5	24.3	1.3	19.9	3.3	4.3	1.9	6.8
BIOS-B	382	19.0	60.0	3.4	40.9	9.5	11.6	9.9	8.4
BIOS-A	9.5	0.8	102	5.4	86.5	15.2	13.3	10.2	9.4
Plant-based									
REED	413	9.9	0.7	7.3	3.6	0.9	0.2	0.1	6.0
REED-B	546	14.6	3.0	24.2	13.8	3.3	6.6	1.2	8.6
REED-A	24.6	0.1	11.2	88.5	47.4	11.0	4.1	0.9	10.2
RICE	381	4.0	0.6	1.9	1.1	0.4	0.2	0.2	7.2
RICE-B	495	7.7	1.6	4.6	3.7	1.2	2.1	1.2	9.1
RICE-A	41.3	1.1	8.7	24.5	15.3	4.4	2.6	1.4	10.0
COCA	453	5.3	1.1	6.3	2.6	1.6	0.8	0.1	6.5
COCA-B	633	6.5	2.4	19.2	6.0	2.7	2.2	1.4	8.5
COCA-A	56.4	1.4	15.8	82.5	36.5	23.7	6.6	0.9	10.7

-B* and -A* denote biochar and ash from the pyrolysis and incineration, respectively, of the feedstock.

2.4. Phosphorus extractions

The P fertiliser potential of all feedstock, biochar and ash materials was assessed by a single extraction of 0.2-g samples in 2% formic acid (FA-P), 2% citric acid (CA-P) and 1 M neutral ammonium citrate (NAC-P) at a 1:100 w/v ratio at room temperature, after dispersing with ultrasonification for 10 min (Rajan et al., 1992; Wang et al., 2012). Each extraction was conducted on three replicate samples. Consistent with the methodology of Wang et al. (2012), the extraction (end-over-end shaking) period for the FA- and CA-P determinations was 30 min, whilst that for NAC-P was 24 h (Mackay et al., 1990). The sonification step was included in the extraction protocol to assist dispersion of the materials in the extractant, especially those with hydrophobic properties and / or with sparingly soluble Fe- and Ca-bound P compounds (Wang et al. 2012). All extractant-solid suspensions were centrifuged at 10000 × *g* for 15 min and suction filtered through a 0.45-µm membrane. Orthophosphate concentration in the filtered extracts was determined using the colorimetric method of Murphy and Riley (1962).

2.5. Phosphorus fractionation

A modified, sequential P-fractionation procedure was used to extract P in the feedstock, biochar and ash materials (Hedley et al., 1982). A 0.5-g sample was extracted sequentially by 30 mL of deionised water, 0.5 M $NaHCO_3$ at pH 8.5, 0.1 M NaOH and 1 M HCl in triplicate. Each fractionation step was performed on a reciprocal shaker for 16 h at room temperature. Following each step, the extract was centrifuged at 10000 × *g* for 20 min and suction filtered through a 0.45-µm membrane. Total P in the extracts (Pt) was measured as orthophosphate (Pi), following digestion of the filtrate with ammonium persulphate (Bowman, 1989). In the filtered $NaHCO_3$ and NaOH extracts, Pi concentration was also measured in a non-digested aliquot; this allowed calculation of organic P (Po) in these two extracts as the difference between the Pt and Pi contents. In all cases, Pi was determined using the colorimetric method of Murphy and Riley (1962).

The sequential P fractions extracted by H_2O, 0.5 M $NaHCO_3$, 0.1 M NaOH and 1 M HCl represent readily labile P, generally labile (weakly adsorbed Pi on mineral surfaces and easily hydrolysable Po compounds), moderately labile P (associated more strongly with carbonates and Fe/Al oxides or in organic particulates), and low labile P (bound in stable Ca-minerals), respectively. Whilst H_2O– and $NaHCO_3$-P are thought to be available to the plant in the short term, NaOH-P is regarded as plant available in the medium term. The HCl extraction represents P that is essentially unavailable for plant uptake (Qian and Jiang, 2014; Li et al., 2018).

2.6. Phosphorus release kinetics

Phosphorus release from the feedstock, biochar and ash materials was investigated according to the procedure of Tran et al. (2017), based on Liang et al. (2014) and others. A 1-g sample of material was shaken with 200 mL deionised water at 180 rpm at 25 °C on a reciprocating shaker. Samples of the water were withdrawn at 0.1, 0.2, 0.5, 1, 6, 12, 24, 48, 72 and 120 h, and suction filtered immediately through a 0.45-µm membrane. Each sample was run in triplicate. Orthophosphate concentration in the filtrate was determined using the colorimetric method of Murphy and Riley (1962).

The kinetics of P release were evaluated using (1) zero-order, (2) pseudo-first- and (3) pseudo-second order models. These models can be presented, respectively, as follows:

$$q_t = a + k_0 t (t \geqslant 6h) \quad (1)$$

$$In(q_e - q_t) = Inq_e - k_1 t \quad (2)$$

$$t/q_t = 1/k_2 q_e^2 + t/q_e \quad (3)$$

where q_t and q_e (mg g^{-1}) are the amounts of P released per unit weight of material at time *t* (h) and equilibrium, respectively; k_0 (h^{-1}) and *a* (mg

g^{-1}) are constants; k_1 (h^{-1}) and k_2 (g $mg^{-1}h^{-1}$) are rate constants of the pseudo-first- and pseudo-second-order of the release process, respectively. In this study, q_e (Equation (2) and k_1 were calculated from the intercept and slope of the plot of $\ln(q_e - q_t)$ versus t, and q_e (in Equation (3) and k_2 were calculated from the intercept and slope of the plot of t/q_t versus t (Qian et al., 2013; Tran et al., 2017).

3. Results and discussion

3.1. Chemical characteristics of materials

Compared with the plant materials, the lower C and predominantly higher mineral contents of the bio-waste feedstocks reflect the high-mineral diets of animals and humans (Table 1). The P contents of the reed, rice, and cocoa samples are similar to previous reports (e.g., Zheng et al. 2013; Gao et al. 2015); the relatively high P content of the cocoa prunings possibly reflects recent P fertiliser history. In almost all cases, dry matter total P (expressed as TP hereafter) and metal contents among the materials increased in the order: feedstock < biochar < ash (Table 1). Generally, the elemental and pH values are within the range reported in other studies of bio-waste and plant-based feedstocks and their derived biochars and ashes (Cantrell et al. 2012; Komiyama et al., 2013; Uchimiya and Hiradate, 2014; Zwetsloot et al., 2014). The corresponding increases in pH are attributed to the thermal treatments removing volatile acidic compounds, leaving behind alkaline metal oxides.

3.2. Phosphorus extractability

As expected, and consistent with previous workers (e.g., Camps-Arbestain et al. 2015), the concentrations of solvent-extractable P in the bio-wastes (g kg^{-1} material) were much higher than those in the plant-based materials (Table 2). In the vast majority of cases, the proportions of extractable P (% TP) also were higher in the bio-waste materials. Amongst the materials, the dominant trend in P solubility (% TP) was biochar > ash > feedstock, with all three solvents following this trend for poultry manure, sewage sludge, reeds and cocoa prunings (Table 2). Formic acid extracted P in this order also from the bone materials. According to the FA extracts, P solubility in the rice husk materials decreased in the order: biochar > feedstock > ash. Essentially, for all types of biomass, P solubility according to the FA and CA solvents is consistently higher in the derived biochar compared with that in the feedstock and corresponding ash materials. This trend is consistent with an increase in acid-soluble salts as organic P bonds in the feedstock are cleaved at pyrolysis temperatures above 250 °C (Wang et al. 2012). However, at the higher combustion temperature, the dominance of crystalline tertiary Ca-P minerals and apatites probably explains the almost consistently lower extractability of P in the ashes compared with biochar (e.g., Christel et al., 2014; Qian and Jiang, 2014).

The extractability of P (% TP) from the bone and all three plant-based feedstocks, as well as their respective biochar and ash products, decreased in the order: FA-P > CA-P > NAC-P; whereas the order followed FA-P > NAC-P > CA-P in the poultry manure and its thermal products (Table 2). Conversely, P extractability from the pig slurry and sewage sludge, and their respective biochar and ash products, decreased in the order: NAC-P > FA-P > CA-P. In the bone-based materials, the relatively high percentage extractability of P with FA (90 – 96%) demonstrates the ability of the buffered acid pH (<3) of this monocarboxylic organic acid to dissolve the primary component of bone – biological apatite, as well as pyrophosphates and highly crystalline Ca-P minerals that are likely forms in the derived biochar and ash (Zwetsloot et al., 2014; Robinson et al., 2018). The lower values and higher range in the solubility of P in the bone materials using citric acid (58 – 75%) is expected. In spite of its metal complexing potential, CA's proton supply is only 72% of that from formic acid, hence reducing its dissolution of tertiary and apatitic forms of calcium phosphate. Nonetheless, similar to FA, CA also may overestimate plant available P in materials with high contents of these types of P compounds (Kratz et al. 2019). The even lower P solubility in neutral ammonium citrate (23—45%) reflects the highly apatitic chemistry of the bone materials and their relative lack of Fe and Al (Table 1). Similar to the bone materials, the higher solubility of the poultry biowastes' P in FA (58 – 82%), compared with that in CA (47 – 68%) and NAC (49 – 71%), is probably explained by the dominance of Ca-P compounds, as reported by Toor et al. (2005) for different poultry manures. The relatively high contents of Fe and Al in the pig and sludge biowastes explains the higher extractability of these materials' P in NAC (Tables 1 and 2). It is well known that the presence of Fe and Al in sewage sludge biochars can reduce P solubility in formic and citric acids, whilst increasing the ability of NAC to solubilise P by forming strong Fe- and Al-complexes (e.g., Wang et al., 2012).

Table 2
Phosphorus extractability of the biomass feedstocks and their derived biochars and ashes in 2% formic acid (FA-P), 2% citric acid (CA-P) and 1 M neutral ammonium citrate (NAC-P). Standard deviation (n = 3) in parentheses.

Sample	FA-P		CA-P		NAC-P	
	g kg^{-1}	% TP	g kg^{-1}	% TP	g kg^{-1}	% TP
Bio-waste						
BONE	94.0 (1.2)	90.4	70.3 (1.2)	67.6	47.1 (1.3)	45.3
BONE-B*	125.1 (2.7)	96.2	97.2 (2.3)	74.8	42.6 (1.4)	32.8
BONE-A*	188.2 (4.6)	92.7	118.1 (3.1)	58.2	45.7 (0.9)	22.5
POUL	7.2 (0.2)	57.5	5.9 (0.1)	47.1	6.2 (0.1)	48.9
POUL-B	28.9 (0.8)	82.0	24.0 (1.0)	68.0	24.9 (0.8)	70.6
POUL-A	32.8 (0.7)	72.6	26.4 (0.6)	58.4	30.3 (0.8)	67.0
PIG	13.7 (0.6)	65.1.0	11.2 (0.8)	54.7	15.2 (0.2)	74.5
PIG-B	37.2 (0.6)	72.8	28.8 (0.6)	56.3	42.2 (1.4)	86.26
PIG-A	60.2 (1.1)	67.01	50.2 (1.2)	54.3	79.7 (1.7)	82.6
BIOS	13.6 (0.1)	55.8	6.7 (0.1)	27.6	13.6 (0.4)	59.29
BIOS-B	39.8 (0.7)	66.3	24.3 (0.6)	40.5	44.2 (1.5)	73.7
BIOS-A	62.2 (1.2)	61.0	34.3 (1.0)	33.6	71.0 (2.0)	69.6
Plant-based						
REED	0.2 (0.0)	32.3	0.2 (0.0)	24.1	0.1 (0.0)	20.0
REED-B	1.5 (0.1)	50.3	1.2 (0.0)	38.9	0.9 (0.0)	33.8
REED-A	5.0 (0.1)	44.2	4.1 (0.2)	36.9	3.4 (0.1)	30.4
RICE	0.2 (0.0)	30.7	0.1 (0.0)	20.5	0.1 (0.0)	18.0
RICE-B	0.6 (0.0)	35.6	0.5 (0.0)	30.7	0.4 (0.0)	27.0
RICE-A	1.9 (0.1)	22.0	1.3 (0.1)	15.4	1.2 (0.0)	14.2
COCA	0.3 (0.0)	24.6	0.2 (0.0)	19.7	0.2 (0.0)	17.6
COCA-B	1.2 (0.0)	50.8	1.0 (0.0)	43.1	0.8 (0.0)	33.6
COCA-A	5.1 (0.0)	32.5	4.4 (0.1)	27.7	3.6 (0.0)	22.5

-B* and -A* denote biochar and ash from the pyrolysis and incineration, respectively, of the feedstock.

A *meta*-analysis, conducted by Camps-Arbestain et al. (2017), of P extractability in biochars produced from a range of biowaste- and plant-based materials indicated that extractability with FA is approximately twice that with NAC. However, a regression analysis of the NAC- against FA-P values among the current biochars, but excluding the bone char, reveals a slope of 1.1; this suggests a much closer similarity between the two solvents (Fig. 1a). Indeed, regression analysis of all feedstocks, biochars and ashes (excluding the three bone materials) also produces a slope close to unity (Fig. 1b). The regression of CA-P against FA-P, either including or excluding the bone materials, is also strongly linear ($P < 0.001$), but produces a slope of only 0.7 (data not presented); this relationship reflects in part the CA solvent's relatively weak proton supply.

The rationale for omitting the three bone materials from the FA-NAC relationships in Fig. 1 rests on the extremely high FA-solubility (>90%) of these materials' biological apatite (Zwetsloot et al. 2014). The strong,

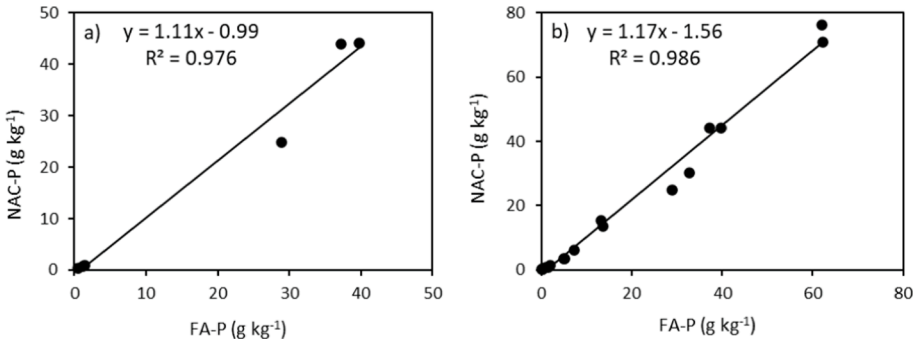

Fig. 1. Relationship between P extractability in 2% formic acid (FA-P) and 1 M neutral ammonium citrate (NAC-P) in a) biochars only and b) biomass feedstocks and their derived biochars and ashes. The bone-based materials are excluded (explanation in text).

almost 1:1 (Fig. 1a), relationship between FA- and NAC-P values among most of the biochars is consistent with the findings of Wang et al. (2012). This agreement is attributed to the relatively long NAC extraction period (24 h) compared with the 1-h extraction used to generate the data analysed by Camps-Arbestain et al. (2017). On this basis, it appears that a 24-h extraction period with NAC might be favourable to the conventional FA extraction when evaluating P fertilizer potential among biochars with a dominant Ca-P chemistry. However, as reviewed by Kratz et al. (2019), NAC may overestimate plant available P by dissolving tertiary forms of calcium phosphate (e.g., whitlockite), as well as Fe/Al precipitates, commonly found both in fresh and pyrolyzed biowastes. Notwithstanding these limitations, it is speculated that a longer extraction period with a pH-neutral, metal complexing agent may solubilise P without dissolving excessive amounts of plant-unavailable tertiary and apatitic Ca-P forms. Carefully standardised plant bioassays are necessary to test these suppositions, especially in comparisons including contrasting materials with highly variable P chemistry.

3.3. Phosphorus fractionation

In spite of the wide-ranging values among the concentrations of P fractions, the sum of the fractions (H_2O–, $NaHCO_3$-, NaOH- and HCl-P) in the different feedstocks, biochars and ashes accounted for the majority of the total P in the materials, with P recoveries ranging from 73 to 97% TP (Table 3). Generally, values for P recovery were higher in the bio-wastes and their derivatives compared with those among the plant-based materials but showed no consistent response to the pyrolysis and incineration treatments (Table 3). Fundamentally, the recalcitrant organic C structure of plant material, and carbon's role in stabilising P at moderate pyrolysis temperatures, might explain the lower P recovery rates for the plant-based feedstocks and their biochars than those for the corresponding biowaste materials (Uchimiya and Hiradate, 2014).

3.3.1. Biowastes

For all four biowastes, the proportion of H_2O-soluble P (%TP) decreased significantly in the order: feedstock > biochar > ash (Fig. 2). In the case of animal bone, Zwetsloot et al. (2014) concluded from P *K*-edge XANES that pyrolysis (reported at temperatures between 350 and 750 °C) increases the crystallinity of the material's characteristically dominant apatite component; this transformation would explain the current sharp decrease in H_2O-Pt upon pyrolysis of the bone. It is likely that the higher combustion temperature (850 °C) would have increased crystallinity further (Glæsner et al., 2019). Moreover, unlike pyrolysis, combustion is unlikely to generate pyrophosphate salts; the possible

Table 3
Concentrations of P fractions in the biomass feedstocks and their derived biochars and ashes. Standard deviation (n = 3) in parentheses.

Sample	H_2O-Pt	$NaHCO_3$-Pi	$NaHCO_3$-Po	NaOH-Pi	NaOH-Po	HCl-Pt	Residual Pt[a]	TP	P recovery
	mg kg^{-1}								%
Bio-waste									
BONE	3141 (160.6)	1154 (55.2)	42 (6.6)	31 (4.8)	10 (2.2)	96,876 (5100.5)	2756	104,010 (4868.7)	97
BONE-B*	1820 (73.6)	520 (16.4)	26 (1.8)	52 (3.0)	26 (2.4)	115,076 (6014.6)	11,960	129,480 (4782.5)	91
BONE-A*	203 (9.4)	406 (16.0)	20 (1.0)	61 (2.9)	20 (3.0)	182,558 (7482.7)	19,691	202,959 (8285.8)	90
POUL	3818 (124.8)	2394 (109.4)	630 (20.8)	504 (21.2)	378 (12.7)	4032 (203.8)	882	12,638 (582.5)	93
POUL-B	1412 114.0)	10,661 (184.8)	530 (27.6)	353 (7.7)	7 (1.6)	20,068 (1074.5)	2118	35,148 (1887.0)	94
POUL-A	54 (3.8)	904 (57.2)	14 (2.0)	9 (1.5)	5 (0.7)	38,782 (1166.3)	5424	45,191 (2006.6)	88
PIG	8364 (244.8)	3468 (155.4)	2244 (147.6)	1632 (111.3)	1040 (49.7)	2013 (97.7)	1632	20,394 (1014.5)	92
PIG-B	1022 (55.4)	17,885 (967.2)	1789 (81.4)	1022 (38.2)	15 (2.4)	26,061 (1210.4)	3066	50,860 (3245.8)	94
PIG-A	185 (10.4)	4625 (138.6)	46 (4.2)	1850 (101.4)	37 (2.6)	66,600 (3372.1)	19,194	92,537 (4285.2)	79
BIOS	559 (27.0)	1701 (94.0)	972 (47.0)	8019 (314.0)	1458 (117.8)	10,206 (447.3)	1409	24,324 (1624.4)	94
BIOS-B	66 (4.2)	1440 (99.6)	24 (2.6)	10,800 (253.7)	1224 (121.6)	39,480 (2146.6)	6960	59,994 (3058.6)	88
BIOS-A	10 (1.8)	512 (15.8)	20 (3.6)	13,312 (234.4)	41 (2.2)	78,234 (3963.8)	10,240	102,369 (4707.7)	90
Plant-based									
REED	126 (6.0)	42 (4.0)	189 (9.6)	42 (3.8)	112 (9.0)	69 (3.2)	119	699 (22.8)	83
REED-B	252 (7.4)	444 (35.2)	33 4.0)	120 (4.8)	30 (3.2)	1380 (83.7)	750	3009 (125.0)	75
REED-A	672 (25.0)	448 (40.4)	4 (1.0)	1568 (109.5)	7 (1.3)	6944 (367.1)	1568	11,211 (467.3)	86
RICE	90 (2.8)	78 (5.4)	132 (5.2)	30 (2.6)	102 (5.6)	27 (1.8)	144	603 (30.9)	76
RICE-B	128 (5.6)	320 (16.8)	114 (7.4)	66 (3.2)	102 (5.6)	528 (27.5)	336	1594 (66.5)	79
RICE-A	348 (17.2)	696 (18.4)	5 (0.6)	948 (49.0)	4 (0.8)	4350 (174.7)	2366	8718 (438.4)	73
COCA	187 (12.8)	176 (14.6)	264 (10.8)	82 (5.0)	242 (8.8)	22 (3.0)	132	1105 (47.8)	88
COCA-B	288 (11.0)	672 (18.0)	206 (12.2)	216 (11.8)	96 (3.0)	384 (18.3)	528	2390 (99.3)	78
COCA-A	632 (21.6)	1580 (96.2)	11 (2.6)	2212 (86.4)	5 (0.8)	9480 (371.9)	1896	15,816 (801.5)	88

-B* and -A* denote biochar and ash from the pyrolysis and incineration, respectively, of the feedstock.
[a] Residual Pt is calculated by subtracting the sum of the water-, $NaHCO_3$-, NaOH- and HCl-P fractions from the dry matter TP content.

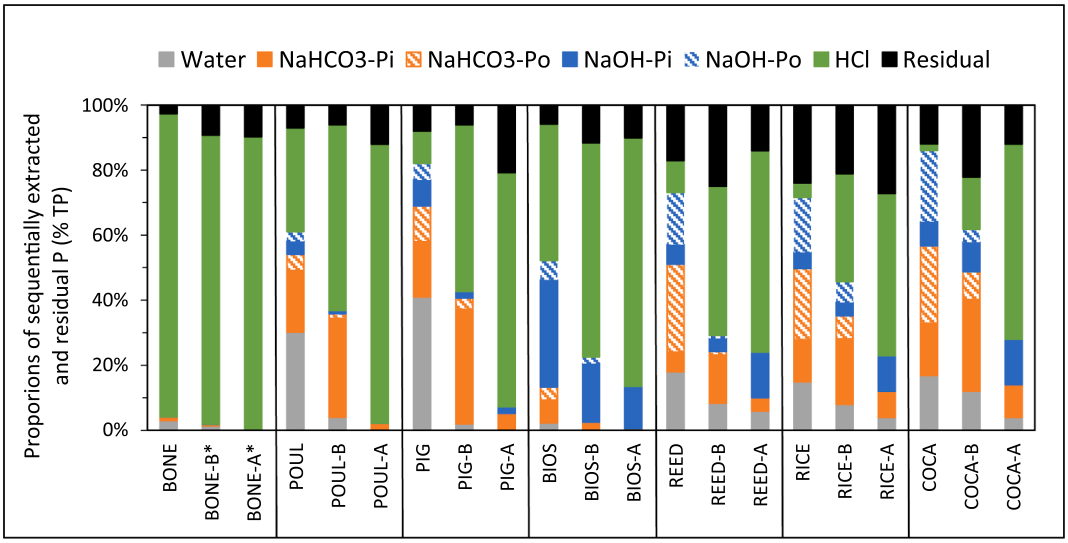

Fig. 2. Fractionation of P in the biomass feedstocks and their derived biochars and ashes, into H_2O–, $NaHCO_3$-, NaOH- and HCl-extractable and residual forms. Residual P is calculated by subtracting the sum of the fractions from the dry matter TP content. -B* and -A* denote biochar and ash from the pyrolysis and incineration, respectively, of the feedstock.

presence of these intermediate species in the bone char, as reported by Robinson et al. (2018), also might contribute to the difference in H_2O-Pt between the bone char and ash.

The H_2O-Pt contents of the poultry manure (3.8 g kg^{-1}) and pig slurry (8.4 g kg^{-1}) were markedly higher than those of the other five feedstocks, accounting for as much as 30% and 41%, respectively, of the TP (Table 3, Fig. 2). Water soluble P is widely reported as being relatively high in animal slurries and manures, comprising primary and secondary alkali phosphates from dietary supplements (such as Na_2H-$PO_4{\cdot}xH_2O$ and $CaHPO_4$) as well as readily hydrolysable Po forms, such as phospholipids, DNA and labile monoesters (Leinweber et al., 1997; Toor et al., 2005; Li et al., 2018). Pyrolysis, however, decreased H_2O-Pt in the pig slurry 20-fold to 2% TP, and incineration to only 0.2% TP (Fig. 2). The corresponding H_2O-Pt decreases in poultry manure were 8-fold to 4% TP and 25-fold to 0.12% TP. These steep decreases in the slurry- and manure- H_2O-Pt following thermal treatment, and corresponding increases in HCl-P (Fig. 2), may be attributed to the formation of a complex mixture of amorphous and crystalline calcium phosphates (Uchimiya and Hiradate, 2014). For example, limited solubility of P in slurry- and manure-derived biochars produced around 500 °C has been attributed to precipitation with high concentrations of Ca and Mg to form minerals such as whitlockite and struvite (Sun et al., 2018). Adsorption of P onto the surfaces of precipitated $CaCO_3$ may also explain the decline in H_2O-Pt (Sun et al., 2018). Furthermore, this region of moderate pyrolysis temperature can precipitate nano-sized P-containing crystals that may become incorporated into or occluded by the pyrolytically formed aromatic C structures of the poultry and pig biochars (Uchimiya and Hiradate, 2014).

The extremely low water extractability of the P in the ashes of the poultry manure (0.1% TP) and pig slurry (0.2% TP) is also consistent with the findings of previous workers. For example, at combustion temperatures similar to that in the present study (850 °C), and higher, H_2O-P in animal manure ash ranged between 0 and 2.5% TP (Kuligowski et al., 2008; Huang et al., 2011; Christel et al., 2014). At incineration temperatures $\geq$ 700 °C, the very low water solubility of the P and dominance of HCl-P have been attributed to the formation of water-insoluble tertiary calcium phosphates and / or different forms of apatites (Thygesen et al., 2011; Komiyama et al., 2013; Christel et al., 2014).

In spite of the steep decreases in H_2O-Pt, and increases in HCl-P, pyrolysis increased the $NaHCO_3$-Pi pool from 19% to 30% TP and 17 to 35% TP in the poultry manure and pig slurry, respectively (Fig. 2). The net shift of P into this plant-available pool can be attributed to a combination of organic P decomposition and an increased association of inorganic P with mineral surfaces through weak adsorption reactions (e.g., Liang et al., 2017). Moreover, the current pyrolysis temperature of 500 °C is known to produce labile organic matter which can condense rapidly on the biochar surface (Lu et al., 2013; Qian and Jiang, 2014). This organic matter contains certain carboxyl and hydroxyl groups that may provide additional P retention sites whilst decreasing the P bonding energy and buffer capacity; the net effect is an increase in P availability (Yang et al. 2019). It is also possible, however, that the acidic, colorimetric analysis of the $NaHCO_3$ extracts overestimated the Pi content by hydrolysing pyrophosphates; these P species are known to form at moderate pyrolysis temperatures (e.g., Liang et al., 2017).

Whilst the values for H_2O-Pt in the sewage sludge (559 mg kg^{-1} material and 2.3% TP) were consistent with previous research (e.g., Kratz et al. 2019), they were significantly lower than those in the other three biowaste feedstocks (Table 3, Fig. 2). This relatively low H_2O-Pt in sludge is attributed to the microbiological treatment process that is designed to convert soluble P into intracellular polyphosphate compounds (Mehta et al., 2015). As much as 33% of the TP was recovered in the NaOH-Pi pool, and almost 50% shared between the HCl-P (42%) and residual P (6%) pools. The dominance of adsorbed (NaOH-) and precipitated (HCl-) Pi possibly reflects a high rate of polyphosphate hydrolysis during NaOH extraction and / or the much wider range of metals commonly present in sewage sludge compared to plant and manure feedstocks (data not presented); i.e., additional to the major metals in Table 1. As such, only approximately 13% of the P was recovered as labile P ($NaHCO_3$-Pt); this indicates a relatively low plant availability of the P in the sludge feedstock (Qian and Jiang, 2014). Upon thermal treatment of the sewage sludge, H_2O-Pt decreased further, from 2.3% TP to 0.11 and 0.01% TP in the biochar and ash, respectively (Fig. 2). Pyrolysis probably transformed the soluble P into a combination of sparingly soluble crystalline and amorphous ortho- and pyrophosphate species (Qian and Jiang, 2014; Huang and Tang, 2015; Robinson et al., 2018). Pyrophosphate is known to remain stable in NaOH extracts (Hinedi et al., 1989) and, if hydrolysed to orthophosphate during colorimetric analysis, may explain some of the relatively high NaOH-Pi pool (18% TP) in the biochar. The incineration temperature presumably allowed the uninhibited formation of insoluble Ca- and Mg-P compounds (Qian and Jiang, 2014). The high incineration temperature (850 °C) probably transformed most of the P, including some of the Fe- and Al-bound P (NaOH-Pi) into insoluble, crystalline Ca-P (HCl-extractable)

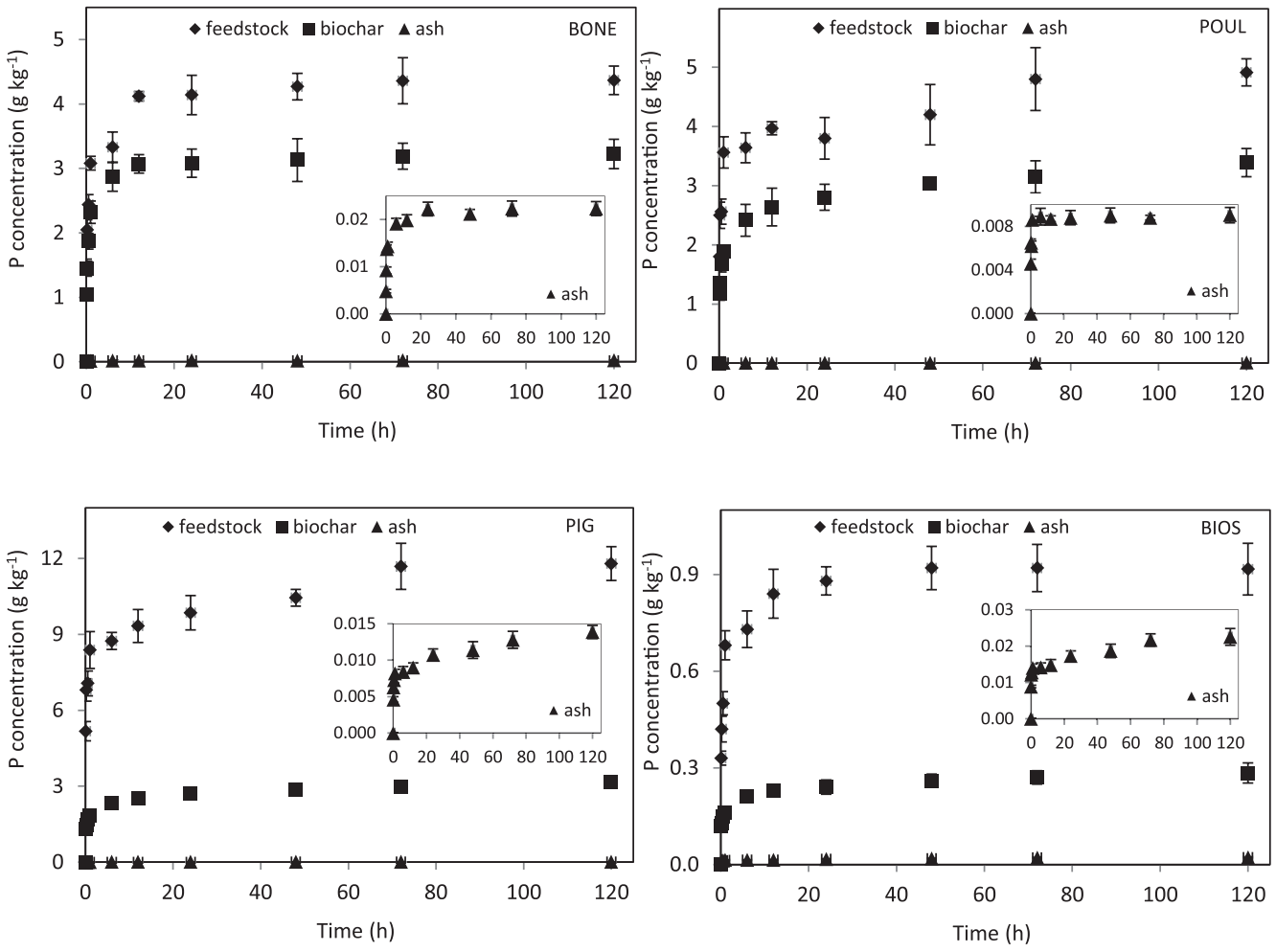

Fig. 3. P release from the biomass feedstocks and their derived biochars and ashes. The subplots for the four biowaste materials show P release from the ashes with an enlarged y axis. Error bars represent ± SE (n = 3).

minerals, such as apatite, stanfieldite and the metaphosphate - $Ca(PO_3)_2$ (Qian and Jiang, 2014; Li et al., 2015).

3.3.2. *Plant-based*

Water-soluble P concentrations in the plant-based feedstocks (90 – 187 mg kg^{-1}) were markedly lower and less variable than those among the biowastes (559–8364 mg kg^{-1}) (Table 3). A similar contrast between the two categories of feedstock was observed in their $NaHCO_3$-Pi pools, ranging in the former from 42 mg kg^{-1} (REED) to 176 mg kg^{-1} (COCA) compared with 1154 mg kg^{-1} (BONE) to 3468 mg kg^{-1} (PIG) among the bio-wastes (Table 3). As indicators of the most plant-available pools of Pi, the H_2O-Pt and $NaHCO_3$-Pi data clearly demonstrate the relative inferiority of the plant-based feedstocks as P fertilisers. However, when expressed as proportions of the feedstock TP content, the sum of labile Pi (H_2O-Pt + $NaHCO_3$-Pi) accounted for as much as 24% TP, 28% TP and 33% TP in the reed, rice and coca feedstocks, respectively.

In the $NaHCO_3$ and NaOH extracts of the three plant-based feedstocks, Po accounted for the majority of the total P (Pt) fraction, ranging from 60% to 82% of the $NaHCO_3$-Pt, and 73% to 77% of the NaOH-Pt (Fig. 2). This dominance of Po over Pi reflects the high levels of phytic acid (60–80% TP) in the seeds and grains of plant material (Uchimiya and Hiradate, 2014).

Similar to the effects of thermal treatment on the biowaste feedstocks, pyrolysis and incineration of the plant-based materials markedly decreased their proportions of TP as H_2O-Pt (Fig. 2); these changes are probably attributed to the formation of increasingly crystallized, less soluble Ca- and Mg-P minerals at temperatures above around 500 °C (e.g. Zheng et al., 2013; Xu et al., 2016). These P transformations would explain the approximately 5- to 8-fold increases in HCl-P among the three plant-based feedstocks following pyrolysis. Similar to the current study, Xu et al. (2016) reported H_2O-P values of 6.4%, 5.3% and 10.9% TP in the biochars of maize straw, wheat straw and peanut husk, respectively, produced at 600 °C. It is important to remember that the recorded increases in the concentration of H_2O-Pt (g kg^{-1} material), and other P fractions, simply reflect the marked positive effect of the thermal treatments on TP content (Table 3).

The higher water solubility and extractability of labile P among several of the biochars and ashes derived from plant materials compared with those from the biowastes can be attributed to the formation of water soluble pyrophosphates (e.g. $Na_4P_2O_7$) and / or sparingly soluble dicalcium phosphates (e.g. monetite and brushite) in the former (Xu et al., 2016). Whilst overall there is a marked migration of P towards non-labile pools, the current data suggest that moderate pyrolyis temperatures redistribute some of the H_2O-P in the plant-based feedstocks into the less mobile, yet plant-available, $NaHCO_3$-Pi pool (Fig. 2). Other likely sources of the increased $NaHCO_3$-Pi include Po forms, some of which are known to thermally decompose at moderate temperatures. Similar conclusions were drawn by Xu et al. (2016), who observed that peak recoveries of $NaHCO_3$-Pi (15 – 25% TP) in plant-based biochars (wheat straw, maize straw and peanut husk) coincided with the

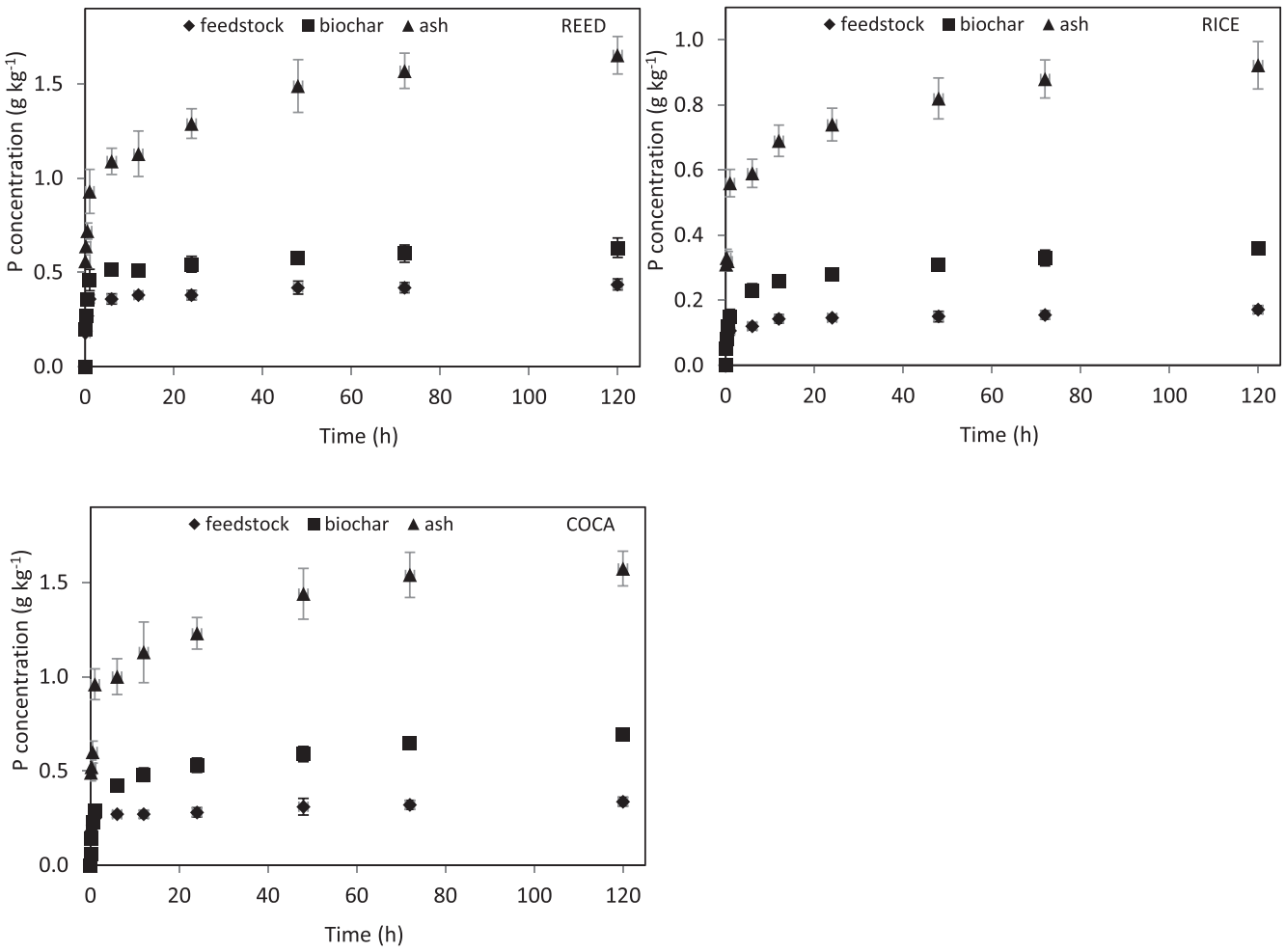

Fig. 3. (*continued*).

moderate pyrolysis temperatures in the region of 300 to 400 °C. Similar to the livestock waste biochars, it is also possible that the acidic colorimetric analysis of the $NaHCO_3$ extracts overestimated Pi by hydrolysing pyrophosphates.

3.4. P release kinetics

Orthophosphate release from the biomass feedstocks and their derived biochars and ashes as a function of time is illustrated in Fig. 3. For all 21 materials, P release was very rapid during the initial 6 – 12 h. Comparable with previous workers, most of the total release (77–99%) occurred in the initial 24 h, followed by a very slow-release phase after 48 h (Liang et al., 2014; Tran et al., 2017; Sun et al., 2018). For all four biowastes, the rate and extent of P release per unit weight of material decreased in the order: feedstock > biochar > ash (Fig. 3); this trend is consistent with the decreasing water solubility of the P per unit weight of material (Table 3). Conversely, for each of the plant-based materials, P release decreased in the order: ash > biochar > feedstock (Fig. 3).

The values of $q_{e,cal}$, rate constants (k_1 and k_2) and correlation coefficients (R^2) for the pseudo-first and -second order models are shown in Table 4. For all 21 materials, the calculated qe ($q_{e,cal}$) values for P released using the pseudo-second-order model agreed with the experimental qe ($q_{e,exp}$) values more closely than those using the pseudo-first-order model. According to the fitted R^2 and p values, the pseudo-second order model clearly provided the best fit with the experimental data (Table 4, Table S1). Example linear plots of the pseudo-second-order model are shown for P release both from the poultry manure and rice husk feedstocks and their corresponding biochar and ash materials (Figs. S1 and S2). Assuming that P release proceeds through two steps – surface disintegration / dissolution / desorption reactions followed by solute diffusion – it appears that this sequence of fundamental processes can be expressed very accurately ($R^2 \geq 0.992$, $p < 0.001$) by the single second-order kinetic constant, k_2.

Among all seven feedstocks and their biochars, the rate constant k_2 decreases curvilinearly with increasing labile Pi (H_2O-Pt + $NaHCO_3$-Pi); this indicates that with increasing content of labile P, the rate of P release is less affected by time (Fig. 4). However, the relatively steep portion of this relationship reveals that the plant-based feedstocks and biochar data are better fitted with a linear model ($R^2 = 0.781$, $p < 0.05$); whereas, the corresponding bio-waste materials are better fitted by a power function ($R^2 = 0.703$, $p < 0.01$). The rationale for omitting the ash materials from this data analysis rests on the extraordinarily high values for the biowaste ash P release constant, k_2 (23.4 to 429.9 kg $g^{-1}h^{-1}$). Whilst expected, values of this magnitude do not support discussion of the P release processes from ash. Whereas the relationships for feedstocks and biochars suggest that the diminished effect of time on P release rate from the plant-based feedstocks and biochars is especially sensitive to labile P, whilst it is more likely that diffusion is the rate controlling step for P release from the biowaste feedstocks and biochars.

4. Conclusions

Among all of the P-rich biowastes, both the solubility and release rate of P in water consistently decreased in the order: feedstock > biochar > ash. As such, in agricultural areas where high-P biowastes may be the dominant P fertiliser source, thermal treatment clearly provides an

Table 4
Parameters of pseudo-first-order and pseudo-second-order models.

Sample	Pseudo-first-order			Pseudo-second-order			$q_{e,exp}$
	$q_{e,cal}$ g kg^{-1}	k_1 x $10^{-3}h^{-1}$	R^2	$q_{e,cal}$ g kg^{-1}	k_2 kg $g^{-1}h^{-1}$	R^2	g kg^{-1}
Bio-waste							
BONE	1.93	75	0.916	4.39	0.2953	0.999	4.37
BONE-B*	1.11	54.5	0.765	3.22	0.5218	0.999	3.22
BONE-A*	0.01	77	0.763	0.022	58.9077	0.999	0.0223
POUL	2.40	38.1	0.820	4.89	0.0953	0.995	4.91
POUL-B	1.73	31.3	0.831	3.35	0.1481	0.997	3.39
POUL-A	0.00	44.3	0.399	0.01	429.9	0.999	0.009
PIG	5.64	47.3	0.864	11.79	0.0	0.997	11.79
PIG-B	1.51	32.5	0.830	3.14	0.2	0.998	3.17
PIG-A	0.01	27.3	0.870	0.01	23.4	0.992	0.0139
BIOS	0.47	118	0.866	0.92	1.7	0.999	0.92
BIOS-B	0.14	35.2	0.856	0.28	2.1	0.998	0.28
BIOS-A	0.01	33.6	0.877	0.02	15.1	0.992	0.0225
Plant-based							
REED	0.16	38.8	0.738	0.43	2.1	0.999	0.44
REED-B	0.27	33.8	0.766	0.63	1.1	0.988	0.63
REED-A	2.60	6.6	0.694	1.65	0.2	0.996	1.65
RICE	0.08	26.7	0.696	0.17	3.2	0.996	0.171
RICE-B	0.23	32	0.872	0.36	1.0	0.995	0.36
RICE-A	1.45	6.8	0.663	0.92	0.5	0.997	0.92
COCA	0.14	32.3	0.784	0.33	1.9	0.998	0.34
COCA-B	0.47	34.9	0.916	0.69	0.4	0.995	0.69
COCA-A	2.89	6	0.692	1.58	0.3	0.997	1.57

-B* and -A* denote biochar and ash from the pyrolysis and incineration, respectively, of the feedstock.

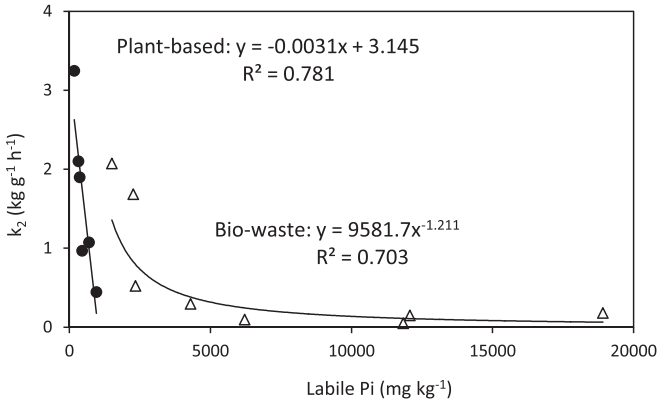

Fig. 4. Relationships between labile Pi content and the pseudo-second order P release constant (k_2) among the bio-waste- (Δ) and plant-based (●) feedstocks and derived biochars.

opportunity to further enrich and standardise biowaste P status whilst reducing the initial, rapid loss of water-soluble P from the amended land to local, biologically sensitive water bodies.

Whilst the thermal transformations appear to support the use both of biowaste biochars and ashes as secondary P resources, it is argued that weak acid extractions may overestimate the P fertiliser value of Ca-P dominated biochars and ashes, especially in calcareous soils. On the other hand, it is also feasible that water solubility and the pseudo second-order release kinetics underestimate the plant-available P pool in these materials. With specific reference to poultry manure and pig slurry, the case for biochar as a viable P fertiliser is strongly supported by the apparent shift of P from the water-soluble to plant-available ($NaHCO_3$-Pi) pool. Indeed, similar trends in the redistribution of P into less mobile yet potentially plant-available pools were evident following pyrolysis of all three low-P feedstocks. Hence, for P-deficient soils in low-input agriculture, some plant-based biochars could be considered as alternative P fertilisers. The current findings provide a novel demonstration of the potential importance of pyrolysis at moderate temperatures both in decreasing runoff P losses from high-P manures and slurries, but also in maintaining or possibly prolonging the fertilizer value of low-P materials.

Declaration of Competing Interest

The authors declare that they have no known competing financial interests or personal relationships that could have appeared to influence the work reported in this paper.

Data availability

No data was used for the research described in the article.

Acknowledgements

This research did not receive any specific grant from funding agencies in the public, commercial, or not-for-profit sectors. The authors are grateful to Mr Xianze Xu, Ms Marta O'Brien and Ms Anne Dudley for their assistance with the chemical analysis.

Appendix A. Supplementary data

Supplementary data to this article can be found online at https://doi.org/10.1016/j.wasman.2023.10.012.

References

Bowman, R.A., 1989. A sequential extraction procedure with concentrated sulfuric acid and dilute base for soil organic phosphorus. Soil Sci. Soc. Am. J. 53, 362–366.

Camps-Arbestain, M., Amonette, J.E., Singh, B.P., Wang, T., Schmidt, H.P., 2015. A biochar classification system and associated test methods. In: Lehmann, J., Joseph, S. (Eds.), Biochar for Environmental Management - Science, Technology and Implementation. Routledge, Oxon, pp. 165–193.

Cantrell, K.B., Ducey, T., Ro, K.S., Hunt, P.G., 2008. Livestock waste-to-bioenergy generation opportunities. Bioresour. Technol. 99, 7941–7953.

Cantrell, K.B., Hunt, P.G., Uchimiya, M., Novak, J.M., Ro, K.S., 2012. Impact of pyrolysis temperature and manure source on physicochemical characteristics of biochar. Bioresour. Technol. 107, 419–428.

Chan, K.Y., Xu, Z., 2009. Biochar: Nutrient properties and their enhancement. In: Lehmann, J., Joseph, S. (Eds.), Biochar for Environmental Management – Science and Technology. Routledge, London, pp. 67–84.

Christel, W., Bruun, S., Magid, J., Jensen, L.S., 2014. Phosphorus availability from the solid fraction of pig slurry is altered by composting or thermal treatment. Bioresource Technol. 169, 543–551.

Cordell, D., White, S., 2011. Peak phosphorus: clarifying the key issues of a vigorous debate about long-term phosphorus security. Sustainability 3, 2027–2049.

Gao, H., Zhou, C., Wang, R., Li, X., 2015. Comparison and evaluation of co-composting corn stalk or rice husk with swine waste in China. Waste Biomass Valoriz. 6, 699–710.

Glæsner, N., Hansen, H.C.B., Hu, Y., Bekiaris, G., Bruun, S., 2019. Low crystalline apatite in bone char produced at low temperature ameliorates phosphorus-deficient soils. Chemosphere. https://doi.org/10.1016/j.chemosphere.2019.02.048.

Gunes, A., Inal, A., Taskin, M.B., Sahin, O., Kaya, E.C., Atakol, A., 2014. Effect of phosphorus-enriched biochar and poultry manure on growth and mineral composition of lettuce (Lactuca sativa L. cv.) grown in alkaline soil. Soil Use Management 30, 182–188.

Hedley, M.J., Stewart, J.W.B., Chauhan, B.S., 1982. Changes in inorganic and organic soil phosphorus fractions induced by cultivation practices and by laboratory incubations. Soil Sci. Soc. Am. J. 46, 970–976.

Hinedi, Z.R., Chang, A.C., Yesinowski, J.P., 1989. Phosphorus-31 magic angle spinning nuclear magnetic resonance of wastewater sludges and sludge-amended soil. Soil Sci. Soc. Am. J. 53, 1053–1056.

Huang, Y., Dong, H., Shang, B., Xin, H., Zhu, Z., 2011. Characterization of animal manure and cornstalk ashes as affected by incineration temperature. Appl. Energy 88, 947–952.

Huang, R., Tang, Y., 2015. Speciation dynamics of phosphorus during (hydro)thermal treatments of sewage sludge. Environ. Sci. Tech. 49, 14466–14474.

Kahiluoto, H., Kuisma, M., Ketoja, E., Salo, T., Heikkinen, J., 2015. Phosphorus in manure and sewage sludge more recyclable than in soluble inorganic fertilizer. Environ. Sci. Tech. 49, 2115–2122.

Komiyama, T., Kobayashi, A., Yahagi, M., 2013. The chemical characteristics of ashes from cattle, swine and poultry manure. J. Mater. Cycles Waste Manage. 15, 106–110.

Kratz, S., Vogel, C., Adam, C., 2019. Agronomic performance of P recycling fertilizers and methods to predict it: a review. Nutr. Cycl. Agroecosyst. 115, 1–39.

Kuligowski, K., Poulsen, T.G., Stoholm, P., Pind, N., Laursen, J., 2008. Nutrients and heavy metals distribution in thermally treated pig manure. Waste Manag. Res. 26, 347–354.

Leinweber, P., Haumaier, L., Zech, W., 1997. Sequential extractions and P-31-NMR spectroscopy of phosphorus forms in animal manures, whole soils and particle-size separates from a densely populated livestock area in northwest Germany. Biol. Fert. Soils 25, 89–94.

Li, W., Feng, X., Song, W., Guo, M., 2018. Transformation of phosphorus in speciation and bioavailability during converting poultry litter to biochar. Front. Sustain. Food Syst. 2, 20.

Li, R., Zhang, Z., Li, Y., Teng, W., Wang, W., Yang, T., 2015. Transformation of apatite phosphorus and non-apatite inorganic phosphorus during incineration of sewage sludge. Chemosphere 141, 57–61.

Liang, Y., Cao, X., Zhao, L., Xu, X., Harris, W., 2014. Phosphorus release from dairy manure, the manure-derived biochar, and their amended soil: effects of phosphorus nature and soil property. J. Environ. Qual. 43, 1504–1509.

Liang, X., Jin, Y., He, M., Niyungeko, C., Zhang, J., Liu, C., Tian, G., Arai, Y., 2017. Phosphorus speciation and release kinetics of swine manure biochar under various pyrolysis temperatures. Environ. Sci. Pollut. Res. https://doi.org/10.1007/s11356-017-0640-8.

Lu, H., Zhang, W., Wang, S., Zhuang, L., Yang, Y., Qiu, R., 2013. Characterization of sewage sludge-derived biochars from different feedstocks and pyrolysis temperatures. J. Anal. Appl. Pyrol. 102, 137–143.

MacKay, A.D., Brown, M.W., Currie, L.D., Hedley, M.J., Tillman, R.W., White, R.E., 1990. Effect of shaking procedures on the neutral ammonium citrate soluble phosphate fraction in fertiliser materials. J. Sci. Food Agric. 50, 443–457.

McKendry, P., 2002. Energy production from biomass (part 2): conversion technologies. Bioresour. Technol. 83, 47–54.

Mehta, C.M., Khunjar, W.O., Nguyen, V., Tait, S., Batstone, D.J., 2015. Technologies to recover nutrients from waste streams: A critical review. Crit. Rev. Environ. Sci. Technol. 45, 385–427.

Murphy, J., Riley, J.P., 1962. A modified single solution method for determination of phosphate in natural waters. Anal. Chim. Acta 27, 31–36.

Negassa, W., Baum, C., Leinweber, P., 2012. Evaluation of agro-industrial by-products as nutrient source for plant growth. Arch. Agron. Soil Sci. 58, 451–460.

Qian, T., Jiang, H., 2014. Migration of phosphorus in sewage sludge during different thermal treatment processes. ACS Sust. Chem. Eng. 2 (6), 1411–1419.

Qian, T., Zhang, X., Hu, J., Jiang, H., 2013. Effects of environmental conditions on the release of phosphorus from biochar. Chemosphere 93, 2069–2075.

Rajan, S.S.S., Brown, M.W., Boyes, M.K., Upsdell, M.P., 1992. Extractable phosphorus to predict agronomic effectiveness of ground and unground phosphate rocks. Fertilizer Research 32, 291–302.

Robinson, J.S., Baumann, K., Hu, Y., Hagemann, P., Kebelmann, L., Leinweber, P., 2018. Phosphorus transformations in plant-based and bio-waste materials induced by pyrolysis. Special Issue "Handling the phosphorus paradox in agriculture and natural ecosystems: Scarcity, necessity, and burden of P". Ambio 47 (suppl. 1), S73–S82.

Römer, W., Steingrobe, B., 2018. Fertilizer Effect of Phosphorus Recycling Products. Sustainability 10, 1166. https://doi.org/10.3390/su10041166.

Schroder, J., 2005. Revisiting the agronomic benefits of manure: A correct assessment and exploitation of its fertilizer value spares the environment. Bioresour. Technol. 6, 253–261.

Sharpley, A.N., McDowell, R.W., Kleinman, P.J., 2001. Phosphorus loss from land to water: integrating agricultural and environmental management. Plant and Soil 237, 287–307.

Sun, K., Qiua, M., Han, L., Jin, J., Wang, Z., Pan, Z., Xing, B., 2018. Speciation of phosphorus in plant- and manure-derived biochars and its dissolution under various aqueous conditions. Sci. Total Environ. 634, 1300–1307.

Thygesen, A., Wernberg, O., Skou, E., Sommer, S.G., 2011. Effect of incineration temperature on phosphorus availability in bio-ash from manure. Environ. Technol. 32, 633–638.

Toor, G.S., Peak, D.J., Sims, J.T., 2005. Phosphorus speciation in broiler litter and turkey manure produced from modified diets. J. Environ. Qual. 34, 687–697.

Tran, Q.T., Maeda, M., Oshita, K., Takaoka, M., 2017. Phosphorus release from cattle manure ash as soil amendment in laboratory-scale tests. Soil Sci. Plant Nutr. 63 (4), 369–376.

U.S. Environmental Protection Agency, 1996. In: Microwave Assisted Acid Digestion of Siliceous and Organically Based Matrices. EPA, Washington, D.C., pp. 1–20

Uchimiya, M., Hiradate, S., 2014. Pyrolysis temperature-dependent changes in dissolved phosphorus speciation of plant and manure biochars. J. Agric. Food Chem. 62, 1802–1809.

Ulrich, A.E., Frossard, E., 2014. On the history of a reoccurring concept: phosphorus scarcity. Sci. Total Environ. 490, 694–707.

Wang, T., Camps-Arbestain, M., Hedley, M., Bishop, P., 2012. Predicting phosphorus bioavailability from high-ash biochars. Plant and Soil 357, 173–187.

Withers, P.J.A., van Dijk, K.C., Neset, T.S.S., Nesme, T., Oenema, O., Rubaek, G.H., Schoumans, O.F., Smit, B., Pellerin, S., 2015. Stewardship to tackle global phosphorus inefficiency: The case of Europe. Ambio 44, 193–206.

Xu, G., Zhang, Y., Shao, H., Sun, J., 2016. Pyrolysis temperature affects phosphorus transformation in biochar: chemical fractionation and 31P NMR analysis. Sci. Total Environ. 569, 65–72.

Yang, X., Chen, X., Yang, X., 2019. Effect of organic matter on phosphorus adsorption and desorption in a black soil from Northeast China. Soil Tillage Res. 187, 85–91.

Zheng, H., Wang, Z., Deng, X., Zhao, J., Luo, Y., Novak, J., Herbert, S., Xing, B., 2013. Characteristics and nutrient values of biochars produced from giant reed at different temperatures. Bioresour. Technol. 130, 463–471.

Zwetsloot, M.J., Lehmann, J., Solomon, D., 2014. Recycling slaughterhouse waste into fertilizer: how do pyrolysis temperature and biomass additions affect phosphorus availability and chemistry? J. Sci. Food Agric. 95, 281–288.